

Optical and Physical studies of Bi Doped Borate Glassy System

M.A. El-Sherbiny^a, A. Samir^b, H. A. Abd El-Ghany^b, F. Metawe^b,
and M.M. El-Okr^a

^a Physics Department, Faculty of Science, Al- Azahr University, Egypt .

^b Engineering Physics and Mathematics Department, Faculty of
Engineering Shoubra, Benha University, Egypt.

Corresponding author: Tel: 01001529111

E-mail address: sherbinypsi@yahoo.com (M.M. El-Okr)

Glasses of composition $x\text{Bi}_2\text{O}_3-(83-x)\text{B}_2\text{O}_3-15\text{Na}_2\text{O}-2\text{MnO}_2$ with ($x = 0, 5, 10, 20$ and 25 mol %) have been prepared by conventional melt quench technique. Characterization of the prepared samples has been achieved by X-ray diffraction (XRD), density and optical measurements. The XRD patterns of all the samples showed broad humps typical for amorphous systems. Density and molar volume have been determined and it is found that both are increased with increasing of Bi_2O_3 content. The effect of Bi_2O_3 content on the optical absorption spectra was investigated in the wavelength range 190-1100nm. The fundamental absorption edge has been identified where it exhibits red shift by increasing Bi_2O_3 content and band tail width follow opposite trend. The optical band gap (E_g) values of the investigated glasses are found to lie in the range 2.40 – 1.90 eV whereas the values of (ΔE_c) lie in the range 0.66 – 1.436 eV. Some other physical properties also reported.

1. Introduction

Boric oxide, B_2O_3 , is one of the most important glass formers and flux materials [1-4]. It is a particularly suitable optical material because of its high transparency, low melting point, high thermal stability, different coordination numbers, easy for fabrication, shaping and mass production [5-7].

Bismuth oxide, Bi_2O_3 , cannot be considered as network former because of the small field strength of Bi^{3+} ion, however in combination with B_2O_3 , glass formation is possible in a relatively large composition range [8-10]. Borate

glasses containing Bi_2O_3 exhibits high refractive index, large polarizability and high optical basicity. So it has potential applications in the field of glass ceramics, optical and electronic devices, thermal and mechanical sensors, smart windows and superconducting materials [11-17]. Manganese ions have strong effect on glass properties such as optical, magnetic and electrical properties [18].

The present work aims to study the effect of replacement of B_2O_3 with Bi_2O_3 content on the physical properties such as density, molar volume, optical behavior in $x\text{Bi}_2\text{O}_3-(83-x)\text{B}_2\text{O}_3-15\text{Na}_2\text{O}-2\text{MnO}_2$ with ($x = 0, 5, 10, 20$ and 25 mol %) glassy system.

2. Experimental

2.1. Glass Preparation

The glass system under investigation has the general formula: $x\text{Bi}_2\text{O}_3-(83-x)\text{B}_2\text{O}_3-15\text{Na}_2\text{O}-2\text{MnO}_2$ with ($x = 0, 5, 10, 20$ and 25mol %) have been prepared by conventional melt-quenching technique. Analytical grade chemicals of Bi_2O_3 , H_3BO_3 , Na_2CO_3 and MnO_2 were used in preparation. Appropriate quantities of the chemicals were mixed in agate mortar and melted in an open porcelain crucible in a programmable electric furnace at the temperature range 1000-1100°C for 1 hour depending on glass compositions. The mixture was shaken frequently to ensure the homogeneity. The molten liquid was quenched in air by pouring onto a preheated brass plate to avoid breaking of the samples due to thermal strains and pressing it quickly with another brass plate. The glasses were then immediately transferred to another furnace kept at 300°C and annealed for 3h in order to eliminate the internal mechanical stress produced by rapid cooling of the melt to room temperature. Apart of the prepared samples were selected and polished carefully with fine emery paper in order to study their optical properties.

2.2. Glass Characterization

The amorphous nature of all samples was firstly examined by X-Ray diffraction (XRD) at room temperature using nickel- filtered $\text{Cu-K}\alpha$ radiation, Philips PW3050/60 diffractometer.

The densities of the glass samples were measured by applying conventional Archimedes method with toluene as the immersion liquid ($\rho_0 = 0.868 \text{ g/cm}^3$) and a single pan electric balance. The density (ρ_{glass}) was calculated using the formula [19].

$$r = \left[\frac{W_{air}}{W_{air} - W_l} \right] r_o \quad (1)$$

where, ρ_0 is the density of the liquid, ρ is the density of the glass sample, W_{air} and W_l are the weight of the glass in air and liquid respectively. The molar volume (V_M) was calculated according to the relation [14].

$$V_M = \frac{M_w}{r_{glass}} \quad (2)$$

where, M_w is the molecular weight of the glass samples. Density data were used to estimate the oxygen packing density (OPD) by using the formula [14].

$$OPD = \frac{r}{M_w} \times n \quad (3)$$

where n is the number of oxygen atoms per unit formula. The ionic concentration (N) of Mn ion can be obtained through [20].

$$N \text{ (ions / cm}^3\text{)} = \frac{x r N_A}{M_w} \quad (4)$$

where x is the mole fraction of transition metal oxide, N_A is the Avogadro's number. Obtained values were used to evaluate other related physical properties:

$$\text{Polaron radius, } r_p \text{ (Å)} = \frac{1}{2} \left(\frac{\pi}{6 N} \right)^{1/3} \quad (5)$$

$$\text{Inter ionic distance, } r_i \text{ (Å)} = \left(\frac{1}{N} \right)^{1/3} \quad (6)$$

$$\text{Field strength, } F \text{ (cm}^{-2}\text{)} = Z / r_p^2 \quad (7)$$

2.3. Optical Measurements

The optical absorption spectra of the glass samples were recorded at room temperature using (JENWAY 6405 UV/Vis Spectrophotometer) in the wavelength range (190 - 1100 nm).

3. Results and Discussion.

XRD patterns of the prepared samples are shown in Fig.(1), the patterns show no sharp peaks but broad humps indicating the amorphous nature of the prepared samples.

The density and molar volume are strongly related to the glass structure, distribution of the structural units, compactness, cross linking. The atomic weight of the constituents play principle role in determining the above mentioned

parameters. Thus, replacement of light elements by heavy ones in the glass can cause an increase in the density that may show a linear dependence on the compositions [17]. The estimated values of the measured density (ρ) as well as the calculated molar volume (V_M) are listed in Table1 and shown in Fig.(2). The obtained results reveal that, the density increases from 2.17 to 4.74 g/cm³, and the molar volume increases from 31.64 to 35.34 cm³/mol. as the Bi₂O₃ content increases at the expense of the B₂O₃ content as shown in Fig.(2). The increase in the density by increasing Bi₂O₃ content is most likely related to the replacement of B (atomic mass 10.811) by Bi (atomic mass 208.98). Generally the molar volume showed; follow opposite pattern to that of density. However, in many cases both follow one common pattern where both increases or decreases by changing the composition. In the present system density and molar volume increases by increasing Bi₂O₃ content. This can be accounted by considering that we have two competing factors, the atomic weights and the number of non-bridging oxygen (NBO) which leads to increase in the molar volume i.e. formation of open structure. This behavior was reported earlier for many glass systems [13,14,17]. The variation of density, molar volume and oxygen packing density, ionic concentration of Mn ion, inter ionic distance, polaron radius and field strength with Bi₂O₃ content are shown in (Figs. 2–6) respectively and listed in Table (1). It is evident that the oxygen packing density (OPD) decreases with increasing of Bi₂O₃ content. In this respect the obtained values of oxygen packing density is consistent with the above explanation. This indicates that the structure becomes less tightly packed and the degree of disorder increases as Bi₂O₃ content increased. This behavior is consistent with results observed in reference [14, 21].

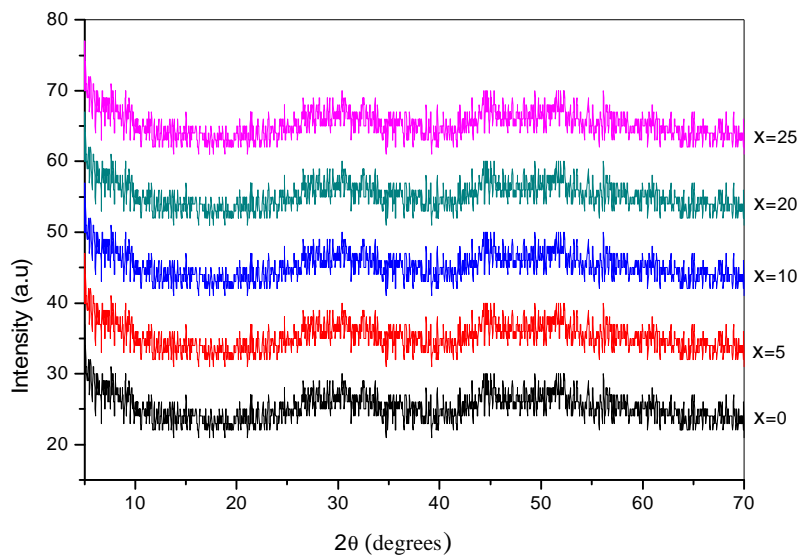


Fig.(1): XRD spectra of the prepared samples.

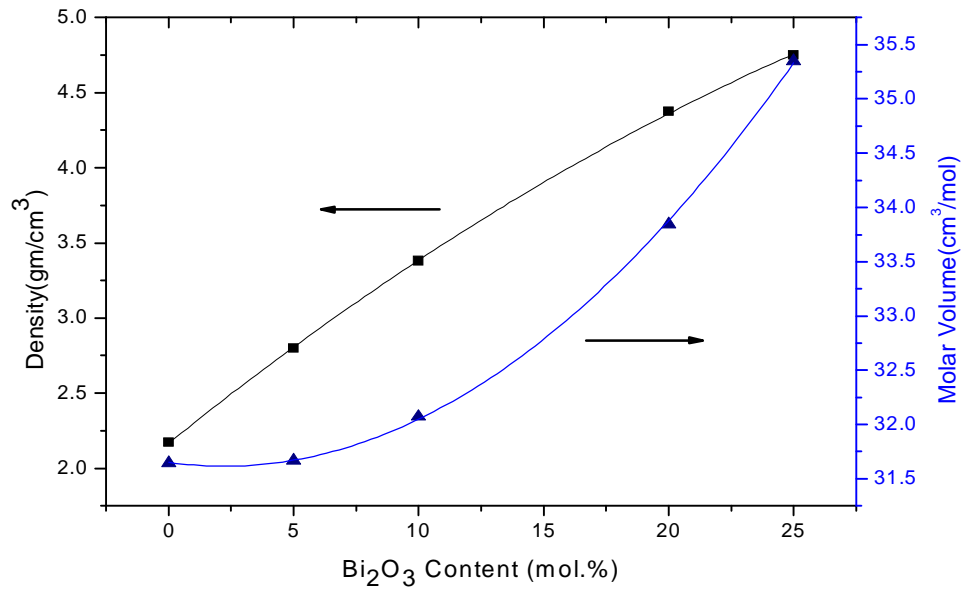


Fig.(2): Variation of density (ρ) and the molar volume (V_M) with composition of Bi_2O_3 .

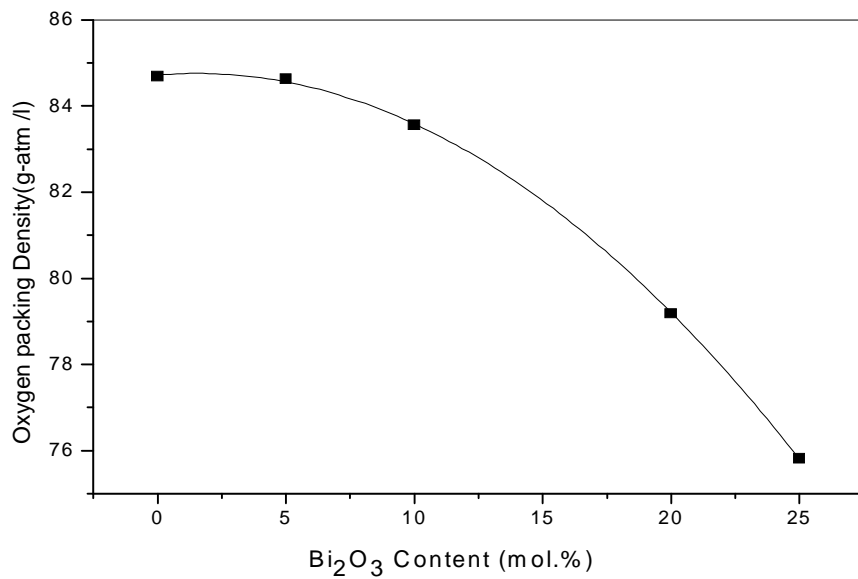


Fig.(3): Variation of oxygen packing density (OPD) with composition of Bi_2O_3 .

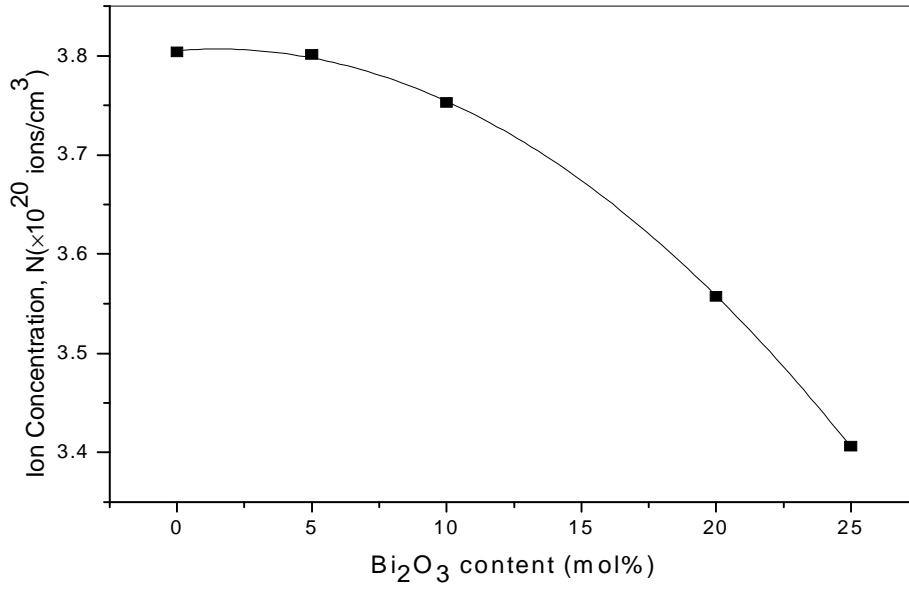


Fig.(4): Variation of Mn ion concentration (N) with composition of Bi₂O₃.

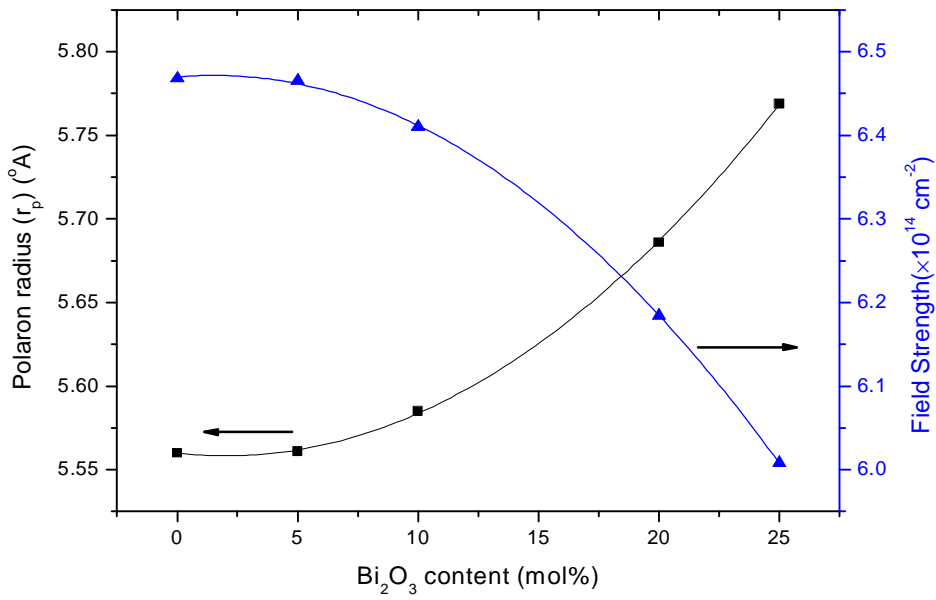


Fig.(5): Variation of Polaron radius (r_p) and Field strength (F) with composition of Bi₂O₃.

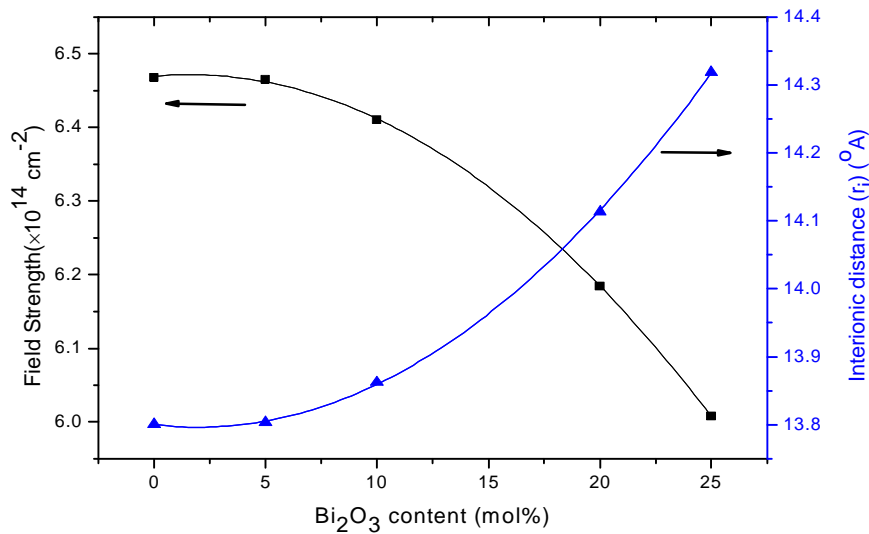


Fig.(6): Variation of interionic distance (r_i) and Field strength(F) with composition of Bi_2O_3 .

Table (1): Physical properties of $x\text{Bi}_2\text{O}_3-(83-x) \text{B}_2\text{O}_3-15\text{Na}_2\text{O}-2\text{MnO}_2$ glassy system .

Physical property	Glass Sample				
	X=0	X=5	X=10	X=20	X=25
Average molecular weight, M (g)	68.81	88.63	108.45	148.08	167.90
Density, ρ (gm/cm^3)	2.17	2.79	3.38	4.37	4.74
Molar volume, V_M (cm^3)	31.64	31.66	32.07	33.84	35.34
Oxygen packing density, OPD($\text{g-atom}/\text{l}$)	84.68	84.62	83.55	79.18	75.81
Mn ion concentration, $N(\times 10^{20} \text{ ions}/\text{cm}^3)$	3.80	3.80	3.75	3.55	3.40
Poloron radius, r_p (Å)	5.56	5.56	5.58	5.68	5.76
Interionic distance, r_i (Å)	13.80	13.80	13.86	14.11	14.31
Field strength, $F(\times 10^{14} \text{ cm}^{-2})$	6.46	6.46	6.41	6.18	6.00
Optical energy gap, E_g (eV)	2.40	2.28	2.08	1.94	1.90
Urbach energy, ΔE_e (eV)	0.66	0.82	1.10	1.37	1.43

3.2. Optical absorption studies

The optical absorption spectra of all the samples in the wavelength range 190–1100 nm are displayed in Fig.(7). The absorption coefficient α (ν), below and near the edge of each curve was determined using the relation [22].

$$a = \left(\frac{1}{d}\right) \ln\left(\frac{I_0}{I}\right) = 2.303 \frac{A}{d} \tag{8}$$

where I_0 and I are the intensities of the incident and transmitted beams, respectively, A is the absorbance and d corresponds to thickness of each sample. The factor $\ln(I_0/I)$ is the absorbance. The relation between $\alpha(\nu)$ and the photon energy of the incident radiation, $h\nu$ was interpreted by Davis and Mott and can be written in general form as [22].

$$\alpha h\nu = B(h\nu - E_g)^n \tag{9}$$

where B is constant called band tailing parameter, E_g is the energy of the optical band gap, n depends on the type of transition (direct or indirect) taking the values $n=2, 3, 1/2, 1/3$ which corresponding to indirect allowed, indirect forbidden, direct allowed, and direct forbidden transitions respectively, n depends also on nature of the material (crystal or amorphous). For amorphous materials, indirect transitions are valid according to Tauc relation i.e. the power part $n=2$. By plotting $(\alpha h\nu)^{1/2}$ as a function of photon energy $h\nu$, the optical energy band gap (E_g) can be determined by extrapolating the linear region of the curve to the $(h\nu)$ axis where $(\alpha h\nu)^{1/2} = 0$ as shown in fig.8. The estimated values are listed in table 1. The relation between $\alpha(\nu)$ and Urbach energy (ΔE_c) is given by the well known Urbach relation [22].

$$a(u) = a_0 \exp[hu/\Delta E_c] \tag{10}$$

where α_0 is constant and ΔE_c is usually interpreted as the width of the tail of the localized states in the band gap and $h\nu$ is the incident photon energy. Urbach plots Fig.() 9 are the plots where the natural logarithm of absorption coefficients, $\ln \alpha$, is plotted against photon energy, $h\nu$. The values of Urbach energy (ΔE_c) were calculated by determining the slopes of the linear portion of the curves and taking their reciprocals. The values of ΔE_c are listed in table 1.

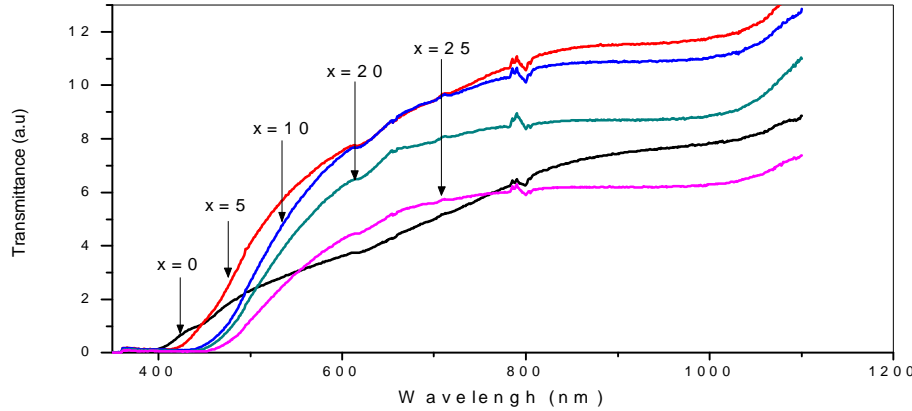


Fig.(7a): Spectral behavior of the $x\text{Bi}_2\text{O}_3-(83-x)\text{B}_2\text{O}_3-15\text{Na}_2\text{O}-2\text{MnO}_2$ glassy system

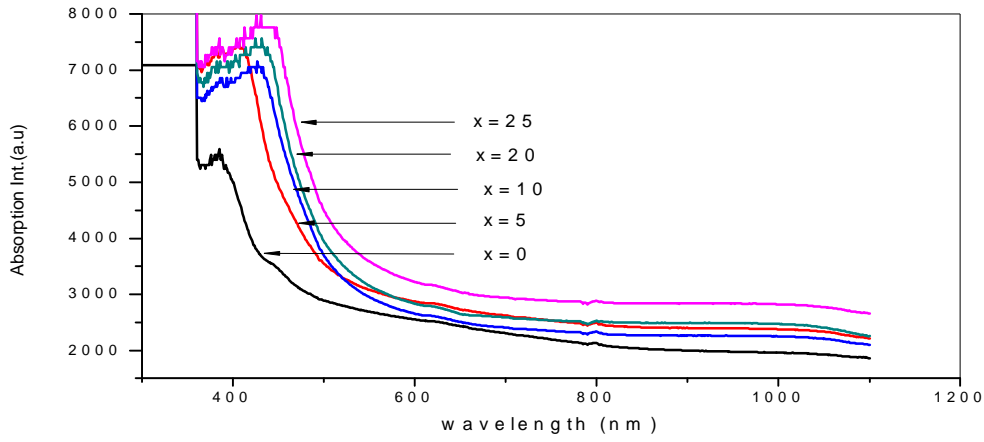


Fig.(7b): Spectral behavior of the $x\text{Bi}_2\text{O}_3-(83-x)\text{B}_2\text{O}_3-15\text{Na}_2\text{O}-2\text{MnO}_2$ glassy system
(a) Transmission (b) Absorption.

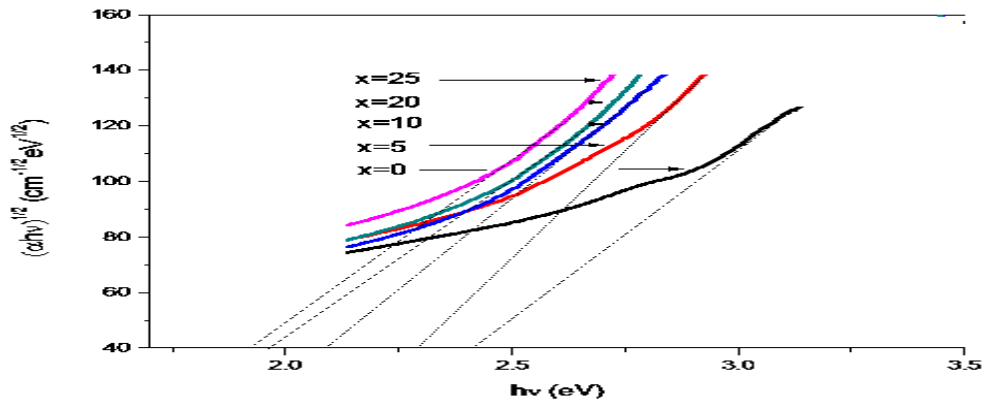


Fig.(8): Tauc's plots for $x\text{Bi}_2\text{O}_3-(83-x)\text{B}_2\text{O}_3-15\text{Na}_2\text{O}-2\text{MnO}_2$ glassy system

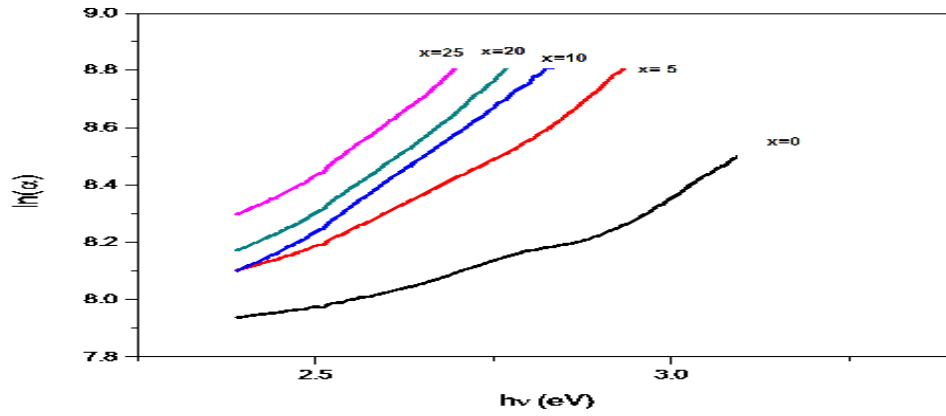


Fig.(9): Dependence of $\ln(\alpha)$ on $(h\nu)$ for $x\text{Bi}_2\text{O}_3-(83-x)\text{B}_2\text{O}_3-15\text{Na}_2\text{O}-2\text{MnO}_2$ glassy system

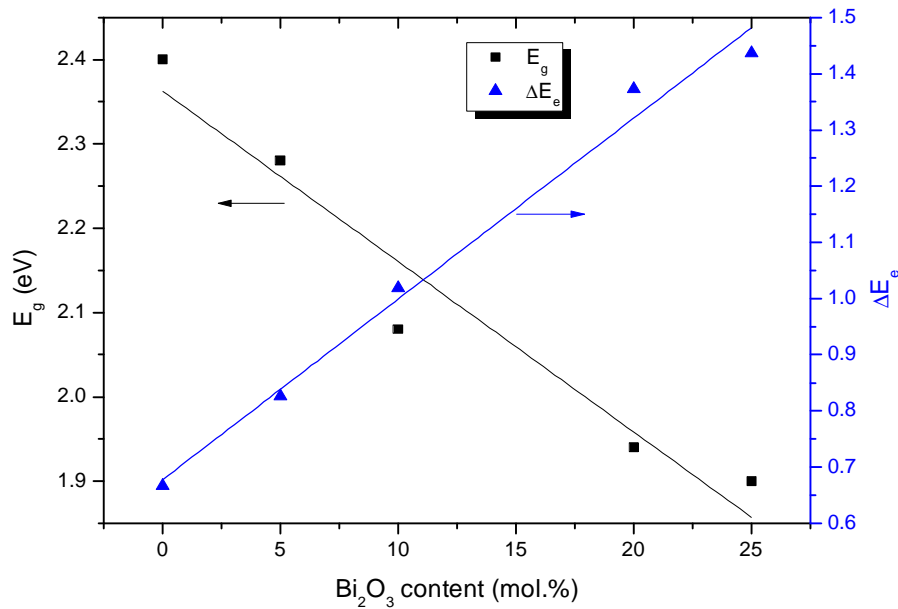


Fig.(10): Variation of optical band gap (E_g) and band tail width (ΔE_e) with composition of Bi_2O_3 .

From the analysis of optical absorption spectra it is found that optical absorption edge is not sharply defined which agree with the non-crystalline nature of the prepared samples. Fig.(9) reveals the indirect transition in the involved absorption mechanism, which is expected seen in glasses. The lack of translation symmetry leads to the fact that the wave vector is not good quantum number i.e. is not conserved. In the present glass system, the shift of the absorption edge or cutoff wavelength to longer wavelength and the decrease of E_g to lower energies with increase in Bi_2O_3 content are related to the progressive increase in the concentration of non-bridging oxygen (NBO) atoms. This increase in turn gives rise to a possible decrease in the number of (B–O–B) bridging oxygen. The shift is attributed to the structural changes due to the replacement of B by Bi. It is possible to assume that as the cation concentration increases, the bridging oxygens (BO) develop bonds with Bi^{3+} which in turn lead to the gradual breakdown of the glass network. This breakdown seems to account for the decrease in the E_g value, i.e., edge shifts to longer wavelengths, as Bi_2O_3 content is increased. Such a decrease in E_g can thus be attributed to decrease in the photon- assisted indirect transitions. A plot of E_g and ΔE_e against Bi_2O_3 content are shown in fig.10. It is observed that E_g and ΔE_e follow opposite trend where the addition of Bi_2O_3 increases the degree of disorder.

4. Conclusions

The glass system under investigation has the general formula: $x\text{Bi}_2\text{O}_3-(83-x)\text{B}_2\text{O}_3-15\text{Na}_2\text{O}-2\text{MnO}_2$ with ($X=0, 5, 10, 20$ and 25 mol %) and has been prepared by conventional melt-quenching technique. The prepared samples have been examined by different techniques including XRD, density and optical absorption spectra. The obtained results allow concluding that:

- The XRD data confirm the amorphous nature of the prepared samples.
- It is observed that the density (ρ) increases with increasing Bi_2O_3 content. This increasing in density is mainly due to the difference in the atomic masses. The molar volume (V_M) increases with increasing Bi_2O_3 content. Such unexpected results can be attributed to the formation of non-bridging oxygen (NBO) i.e. formation of open structure. The larger values of the radii and bond length of Bi_2O_3 , compared to those of B_2O_3 , resulted in a formation of excess free volume, which increase the overall molar volume of the glasses
- The oxygen packing density (OPD) decreases with increasing of Bi_2O_3 content. This indicates that the glass network becomes less tightly packed and the degree of disorder increases as Bi_2O_3 content increases.
- The optical band gap energy (E_g) decreases with increasing of Bi_2O_3 content. This may be attributed to the formation of non-bridging oxygen (NBO). It is observed that (ΔE_c) increases with increasing Bi_2O_3 are due to the addition of Bi_2O_3 increases the disorder of the glass system.

References

1. Isabella-Ioana Oprea, Hartmut Hesse, Klaus Betzler, *Optical Materials*, **26**, 235 (2004).
2. Shashidhar Bal, N.Srinivasa Rao, Syed Rahman, *Solid State Sciences*, **10**, 326 (2008).
3. G. Lakshminarayana, S. Buddhudu, *Spectrochimica Acta Part, A* **63**, 295 (2006).
4. Petru Pascuta, Gheorghe Borodi, Eugen Culea, *Journal of Non-Crystalline Solids*, **354**, 5475 (2008).
5. L. Srinivasa Rao, M. Srinivasa Reddy, M.V. Ramana Reddy, N. Veeraiah, *Physica, B* **403**, 2542 (2008).
6. I. Ardelean, Simona Cora, Raluca Ciceo Lucacel, Octavia Hulpus, *Solid State Sciences*, **7**, 1438 (2005).
7. N. Murase, Y. Kawasaki, A. Tomita, *Journal of Luminescence*, **98**, 301 (2002).
8. S. Simon, I. Ardelean, S. Filip, I. Bratu, I. Cosma, *Solid State Communications*, **116**, 83 (2000).

9. Huiyan Fan, Guonian Wang, Lili Hu, *Solid State Sciences*, **111**, 2065 (2009).
10. Petru Pascuta, Simona Rada, Gheorghe Borodi, Maria Bosca, Lidia Pop, Eugen Culea, *Journal of Molecular Structure*, 924, 214 (2009).
11. A. Dutta, A. Ghosh, *Journal of Non-Crystalline Solids*, **353**, 1333 (2007).
12. Lucian Baia, Razvan Stefan, Wolfgang Kiefer, Jurgen Popp, Simion Simon, *Journal of Non-Crystalline Solids*, **303**, 379 (2002).
13. El Sayed Moustafa, Yasser B. Saddeek, Essam R. Shaaban, *Journal of Physics and Chemistry of Solids*, **69**, 2281 (2008).
14. D. Saritha, Y. Markandeya, M. Salagram, M. Vithal, A.K. Singh, G. Bhikshamaiah, *Journal of Non-Crystalline Solids*, **354**, 5573 (2008).
15. Xinyu Zhao, Xiaoli Wang, Hai Lin, Zhiqiang Wang, *Physica, B* **390**, 293 (2007).
16. S.Sindhu, S.Sanghi, A.Agarwal, V.P.Seth, N.kishore, *Material Chemistry and Physics*, **90**, 83 (2005).
17. Yasser B. Saddeek, Essam R. Shaaban, El Sayed Moustafa, Hesham M. Moustafa, *Physica, B* **403**, 2399 (2008).
18. M. Srinivasa Reddy, G. Murali Krishna, N. Veeraiah, *Journal of Physics and Chemistry of Solids*, **67**, 789 (2006).
19. G. Sharma, V.Rajendran, K.S.Thind, Gagandeep Singh, Amarjit Singh, *Physica, B* **404**, 3371 (2009).
20. A.S. Rao, Y.N. Ahammed, R.R. Reddy, T.V.R. Rao, *Optical Materials*, **10**, 245 (1998).
21. Guojun Gao, Lili Hu, Huiyan Fan, Guonian Wang , Kefeng Li, Suya Feng, Sijun Fan, Huiyu Chen, *Optical Materials*, **32**, 159 (2009).
22. Shashidhar Bale, Syed Rahman, *Journal of Non-Crystalline Solids*, **355**, 2127 (2009).